Hot phonon effects on electron high-field transport in GaAs

1989 J. Phys.: Condens. Matter 1 9401

(http://iopscience.iop.org/0953-8984/1/47/010)

J. Phys.: Condens. Matter 1 (1989) 9401–9412. Printed in the UK

Hot phonon effects on electron high-field transport in GaAs

R Mickevičius and A Reklaitis
Semiconductor Physics Institute of the Lithuanian Academy of Sciences, K Poželos 52, 232600 Vilnius, Lithuania, USSR

Received 5 April 1989

Abstract. An original ensemble Monte Carlo technique for hot phonon problems is applied for the simulation of anisotropic non-equilibrium phonon distributions in momentum space. The dynamics of the coupled non-equilibrium electron–LO-phonon system in electric fields is simulated within the realistic three-valley model of GaAs. Hot phonon effects on the transient and steady-state high-field electron transport as well as on the relaxation of electrically heated electrons are obtained and investigated under various conditions.

1. Introduction

Hot LO phonon generation during the relaxation of hot photoexcited electron–hole plasma in polar semiconductors has been observed experimentally [1–7] and studied theoretically using the ensemble Monte Carlo (EMC) technique [8–13]. It was shown in [4, 8] that hot phonons significantly increase the electron energy relaxation time. On the other hand, hot phonons reduce the photoexcited level depopulation time and modify the transient optical properties [12]. The obtained effects have raised the problem of the roles of hot phonon in electron high-field transport. The first estimations of this role were made in [14, 15] in the framework of the one-valley parabolic band and heated displaced Maxwellian electron distribution model. The case of the two-valley model of GaAs was studied in [16] by the EMC. The hot phonon effects on electron steady-state transport have been obtained.

In the present paper the original EMC [11] is applied for the simulation of anisotropic phonon distributions. The LO phonon 'heating' in electric fields is studied within the realistic three-valley $\Gamma - L - X$ model of GaAs [17, 18]. The hot phonon effects both on the transient and steady-state electron transport are investigated.

2. Method

The Monte Carlo method for the simulation of the non-equilibrium electron–LO-phonon system was proposed in [19] and developed into the general EMC in [11]. This EMC differs from the method of Lugli *et al* [8–10] concerning the determination of phonon wavevector and the electron state after the scattering. The general EMC can be applied for all phonon branches and allows us to take into consideration the modifications

0953-8984/89/479401 + 12 $02.50

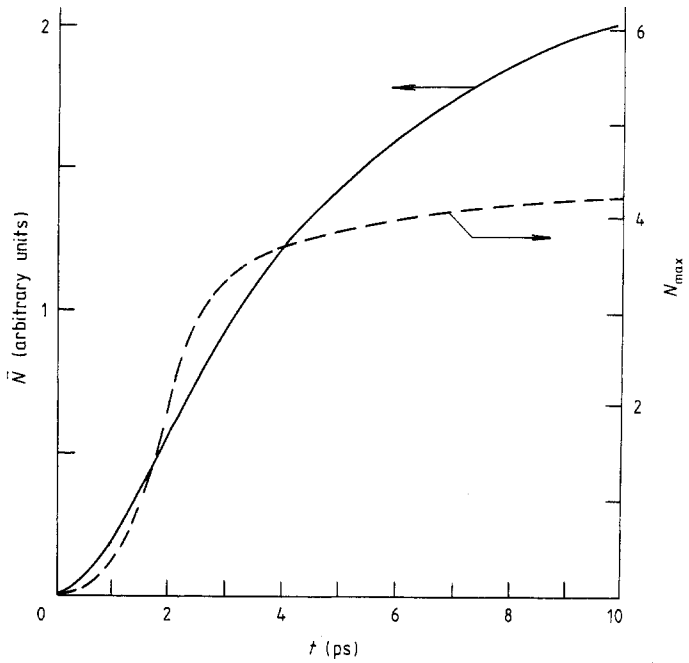

Figure 1. Time evolution of the average non-equilibrium phonon population (left scale) and of the maximum value of the phonon occupation number (right scale) after switching on an electric field for the ionised impurity concentration $n_i = 0$. $E = 1\,\mathrm{kV\,cm^{-1}}$, $T = 77\,\mathrm{K}$, $n = 10^{17}\,\mathrm{cm^{-3}}$.

induced by hot phonons both to the rate of electron–phonon scattering and to the scattering angular dependence. The anisotropy of phonon distribution induced by electric fields can be easily considered by the general method.

Let us consider the field to be applied in the z direction and the conduction band valleys to be spherical. Then transverse to the field directions x and y are equivalent. This allows us to use the two-dimensional cylindrically symmetric grid in $\boldsymbol{q}$-space. The histogram of the two-dimensional phonon distribution $N(q_L, q_T)$, where $q_L = q_Z$, $q_T = \sqrt{q_x^2 + q_y^2}$, is produced at the beginning of the simulation. This histogram is updated after every electron–phonon scattering event by adding to $N(q_L, q_T)$ the following term:

$$\pm \frac{8\pi^2}{2q_T \Delta q_T \Delta q_L + \Delta q_T^2 \Delta q_L} \frac{n}{N_e} \tag{1}$$

where sign '+' corresponds to the emission and '−' to the absorption of the phonon with the wavevector $\boldsymbol{q} = \{q_L, q_T\}$, Δq_T and Δq_L are the steps of the $\boldsymbol{q}$-grid, n is the electron concentration and N_e is the number of simulated particles.

The time is divided into intervals Δt shorter than the average electron–phonon scattering time and much shorter than phonon thermalisation time τ_{ph}. After every interval phonon population is recalculated [11] according to phonon thermalisation. The thermalisation time is assumed to be dependent on equilibrium temperature [20, 21]:

$$\tau_{ph}(T) = \tau_{ph}(0)\left(1 + \frac{2}{(\exp(\hbar\omega/2k_B T) - 1)}\right)^{-1} \tag{2}$$

where $\tau_{ph}(0) = 8\,\mathrm{ps}$ [1, 3, 6, 15] and $\hbar\omega$ is the phonon energy.

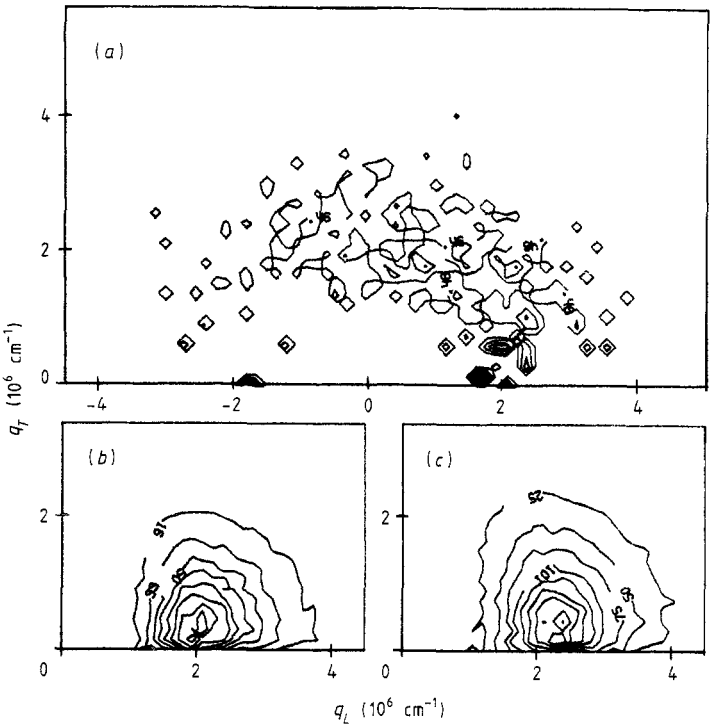

Figure 2. Time evolution of the non-equilibrium phonon distribution in momentum space: isolines of $N(\boldsymbol{q}) \times 10^2$. t = (*a*) 0.25 ps, (*b*) 2.5 ps, (*c*) 5 ps. Other parameters as in figure 1.

The phonon wavevector $\boldsymbol{q}$ and the rate of electron scattering by non-equilibrium phonons are determined in the same way as in [11]. The electron state after the scattering by a LO phonon is defined as $\boldsymbol{k}' = \boldsymbol{k} \pm \boldsymbol{q}$.

The three-valley $\Gamma - L - X$ GaAs model with the parameter set of [11, 18, 21] is used in the simulation. Besides the scattering by LO phonons, the deformation acoustic,

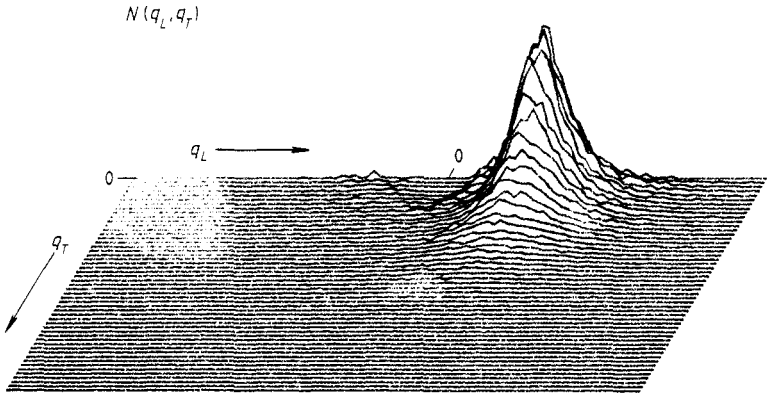

Figure 3. Non-equilibrium phonon distribution in momentum space at t = 5 ps after switching on an electric field. All parameters as in figures 1 and 2.

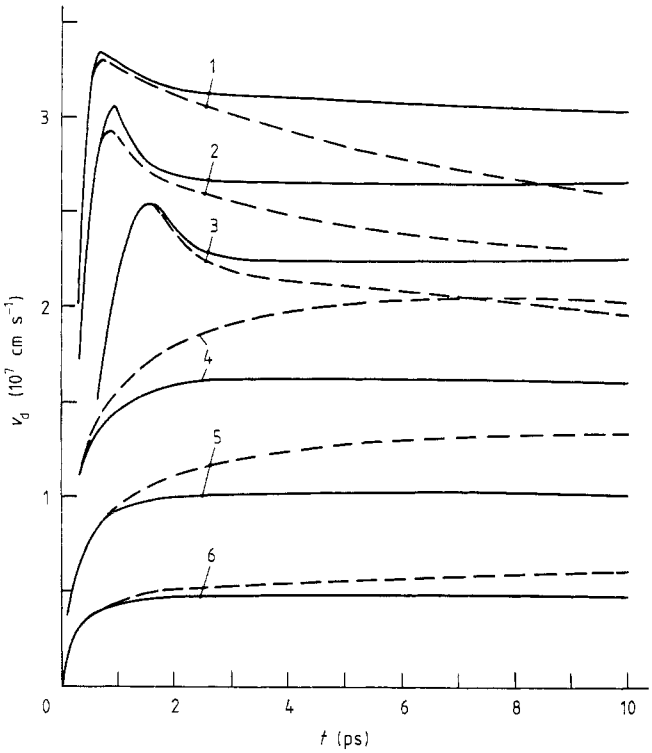

Figure 4. Electron drift velocity transient response to an electric field step switched on at $t = 0$. Curves 1, 2, 3 are calculated for $n_i = 0$, curves 4, 5, 6 for $n_i = 10^{17}$ cm^{-3}; curves 1, 4 for $E = 3$ kV cm^{-1}, 2, 5 for 2 kV cm^{-1}, 3, 6 for 1 kV cm^{-1}. Full curves: without hot phonons; broken curves: with hot phonons. $T = 77$ K, $n = 10^{17}$ cm^{-3}.

ionised impurity and inter-valley scattering of electrons are taken into account. The number of simulated particles $N_e = 10000$ is sufficient for quite an accurate calculation of the drift velocity and the mean energy. The phonon non-equilibrium distributions are calculated using $N_e = 60000$ particles.

3. Results

First we shall simulate the time evolution of non-equilibrium phonon distributions in pure GaAs. Figure 1 represents the time evolution of the maximum value of phonon occupation number N_{max} and of the average (total) phonon population $\bar{N}$ (averaged over all the electronically active q-space volume). It is seen that the maximum value of phonon occupation number saturates faster than the average non-equilibrium phonon population. It means that the second phonon evolution stage is associated with the phonon redistribution in momentum space. This is demonstrated in figure 2. The shape of the non-equilibrium phonon distribution in the second stage of the evolution is shown in figure 3. It is seen from figures 2 and 3 that the non-equilibrium phonon distribution in momentum space is forward displaced. This is a result of the anisotropic angular dependence of polar optical scattering.

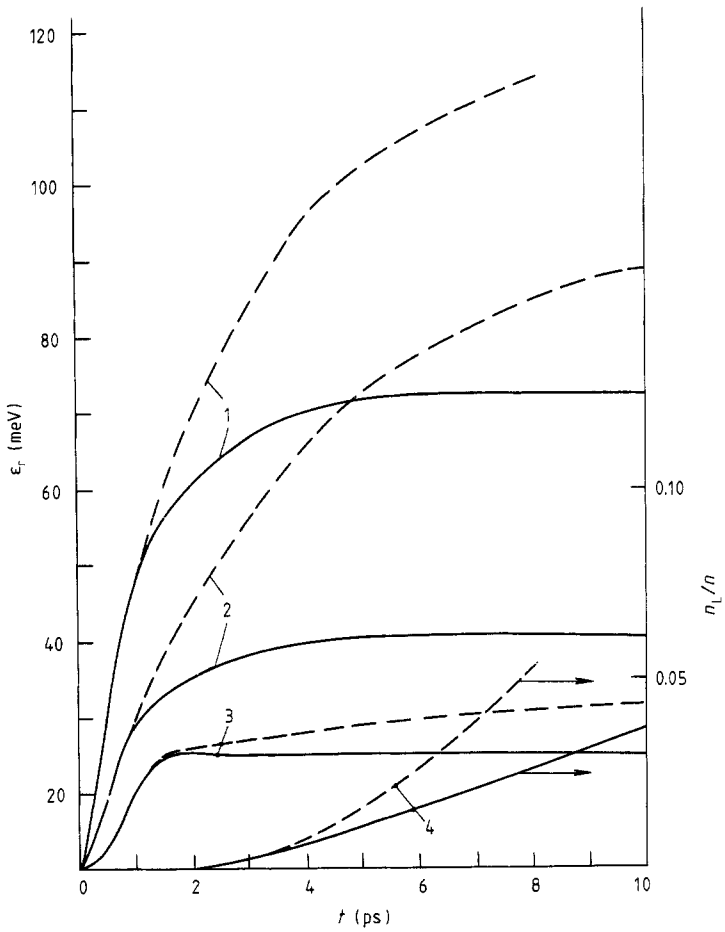

Figure 5. Transient response of the mean electron energy in the Γ valley (left scale) and of the relative population in the L valleys (right scale). Curves 1 and 4 are calculated for $E = 3\,\mathrm{kV\,cm^{-1}}$, $n_i = 0$, curve 2 for $E = 3\,\mathrm{kV\,cm^{-1}}$, $n_i = 10^{17}\,\mathrm{cm^{-3}}$, curve 3 for $E = 1\,\mathrm{kV\,cm^{-1}}$, $n_i = 0$. Full curves: without hot phonons; broken curves: with hot phonons. $T = 77$ K, $n = 10^{17}\,\mathrm{cm^{-3}}$.

Hot phonons in turn can affect the electron transport properties. We have simulated electron transport both in pure (electrons can be injected) and doped GaAs. Figures 4 and 5 demonstrate the electron transient response to an electric field step at low temperature. One can see that in pure GaAs non-equilibrium phonons reduce the electron drift velocity though the mean electron energy increases. On one hand, the electron interaction with non-equilibrium phonons leads to the electron drag due to the forward-displaced phonon distribution in momentum space (hot phonon drag) (figures 2 and 3). On the other hand, this interaction results in the electron momentum randomisation due to the phonon distribution broadening (electron diffusive heating). The diffusive heating reduces the electron drift velocity. As the electron distribution at 77 K is narrow, the diffusive heating predominates over the hot phonon drag effect.

In doped GaAs under the same conditions hot phonons yield the increase of electron drift velocity. This result is associated with the fact that the stimulated phonon absorption

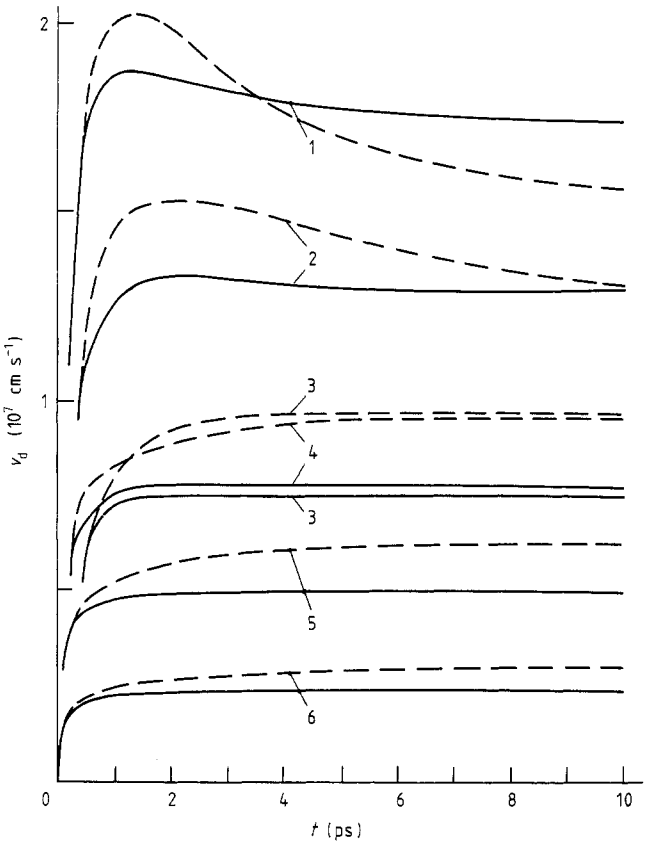

Figure 6. Electron drift velocity transient response. Curves 1, 2, 3: $n_i = 0$, curves 4, 5, 6: $n_i = 5 \times 10^{17}$ cm^{-3}; curves 1, 4 for $E = 3$ kV cm^{-1}, 2, 5 for 2 kV cm^{-1}, 3, 6 for 1 kV cm^{-1}. Full curves: without hot phonons; broken curves: with hot phonons. $T = 300$ K, $n = 5 \times 10^{17}$ cm^{-3}.

promotes electrons to increase their energy and to 'runaway' in energetic space from ionised impurity scattering. The reduction of the ionised impurity scattering increases the electron drift velocity. It is seen from figure 4 that the stimulated reduction of impurity scattering provides a stronger effect in these fields than the electron diffusive heating. The drift velocity increase is insignificant at 1 kV cm^{-1}, but is sufficiently noticeable at 2 and 3 kV cm^{-1}. It is a result of the strong dependence of the ionised impurity scattering rate on electron energy.

It is seen from figure 4 that the electron drift velocity response consists of two stages: the first is governed by the electron distribution function relaxation time under the quasi-equilibrium phonon conditions and the second by the hot phonon thermalisation time which at 77 K is significantly longer: $\tau_{ph} \approx 7$ ps. Therefore, the total response time increases.

Figures 6 and 7 represent the electron transient response to an electric field step at room temperature. As phonon thermalisation time at 300 K is shorter, the hot phonon effects appear at higher electron concentrations. It is seen from figure 6 that the hot phonon stimulated reduction of impurity scattering in doped GaAs manifests itself stronger with the increase of the field (up to 3 kV cm^{-1}).

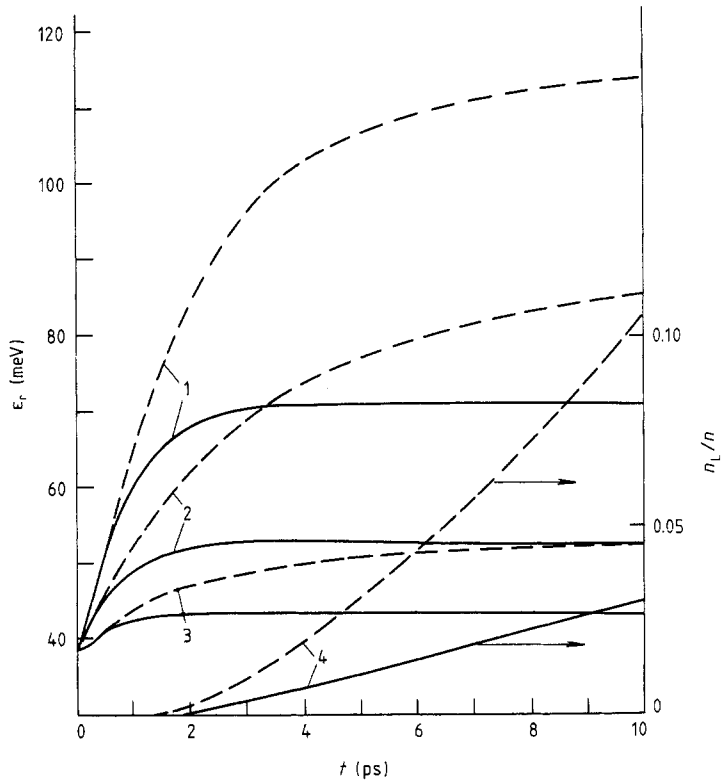

Figure 7. Transient response of the mean electron energy in the Γ valley (left scale) and of the relative population in the L valleys (right scale). Curves 1, 4 for $E = 3$ kV cm^{-1}, $n_i = 0$, curve 2 for $E = 3$ kV cm^{-1}, $n_i = 5 \times 10^{17}$ cm^{-3}, curve 3 for $E = 1$ kV cm^{-1}, $n_i = 0$. Full curves: without hot phonons; broken curves: with hot phonons. $T = 300$ K, $n = 5 \times 10^{17}$ cm^{-3}.

In pure GaAs at room temperature hot phonons also increase the electron drift velocity at the fields below 2 kV cm^{-1}. This is due to the fact that the hot phonon drag at room temperature predominates over the electron diffusive heating.

The most interesting dynamic effect is the hot-phonon-induced velocity overshoot in pure GaAs at 2–3 kV cm^{-1} (figure 6). This overshoot is a result of the hot phonon drag competition with the electron diffusive heating and inter-valley transfer amplification effects. Hot phonons amplify the electron inter-valley transfer because they increase the mean electron energy. With the beginning of the L-valley occupation by electrons ($t \approx 3$ ps, figure 7) the inter-valley transfer amplification effect manifests itself. On the other hand, at the second stage of phonon 'heating' ($t \geqslant 3$ ps) their distribution begins to broaden (figure 2). This leads to the increase of scattering angles and diffusive heating effect. These velocity reducing effects begin to compensate (at 2 kV cm^{-1}) or even predominate (at 3 kV cm^{-1}) over the hot phonon drag at the final stage of the electron transient response. Therefore, at room temperature the hot phonon drag threshold fields correlate with the threshold fields for electron inter-valley transfer.

The electron transient response to the field step 10 kV cm^{-1}, i.e. at the conditions of the intensive inter-valley transfer, is presented in figures 8 and 9. It is seen that hot phonons lead to the electron redistribution between the L and X valleys, whereas the stationary electron population in the Γ valley remains approximately constant. As the

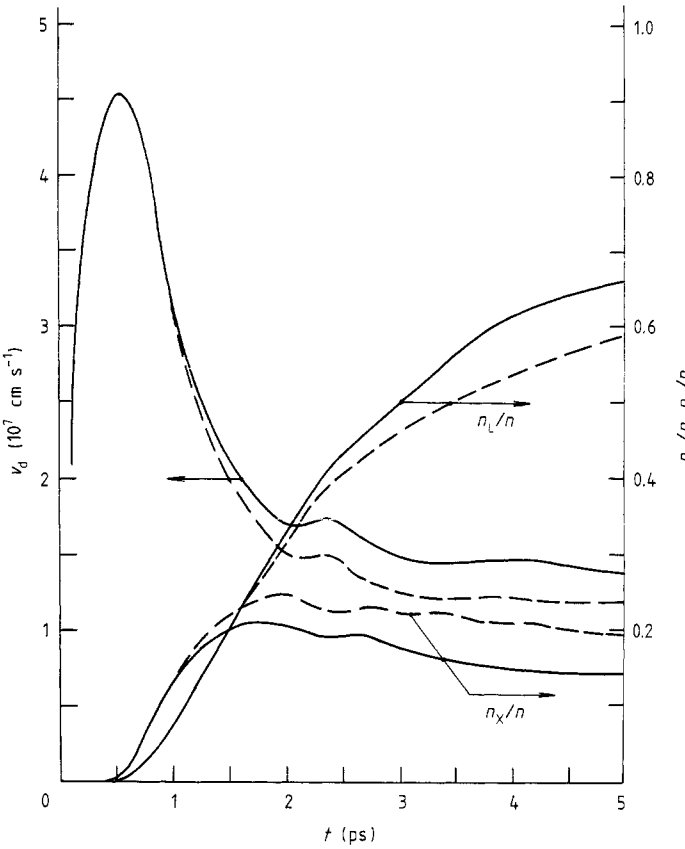

Figure 8. Transient response of the electron drift velocity (left scale) and of the relative population in the L and X valleys (right scale). Full curves: without hot phonons; broken curves: with hot phonons. $T = 300$ K, $n_i = 0$, $n = 5 \times 10^{17}$ cm^{-3}, $E = 10$ kV cm^{-1}.

effective mass of electrons in the X valleys is higher than in the L valleys the resulting hot phonon effect is the drift velocity decrease at the final stage of the response. However, hot phonons do not affect the drift velocity overshoot. The secondary peaks on the drift velocity response are associated with the resonant electron exchange between the Γ and X valleys. One can see from figure 9 that the mean electron energy in the Γ valley is weakly influenced by hot phonons. This is natural, because the electron inter-valley scattering at such fields plays the determinant role.

It is well known from the photoexcited plasma investigations that hot LO phonons result in the increase of hot electron energy relaxation time [4, 5, 8]. Therefore, it is interesting to study the hot phonon role in electrically heated electron momentum relaxation. The drift velocity and non-equilibrium phonon population transient response to a square electric field pulse is plotted in figure 10. One can see that hot phonons yield the slower drift velocity (momentum) relaxation. This is due to the polar character of LO phonons and the non-equilibrium phonon distribution shifted in momentum space. The interaction with the 'shifted' phonons leads to the prolonged relaxation of the drift velocity. The final stage of the drift velocity relaxation is controlled mainly by the hot phonon thermalisation time.

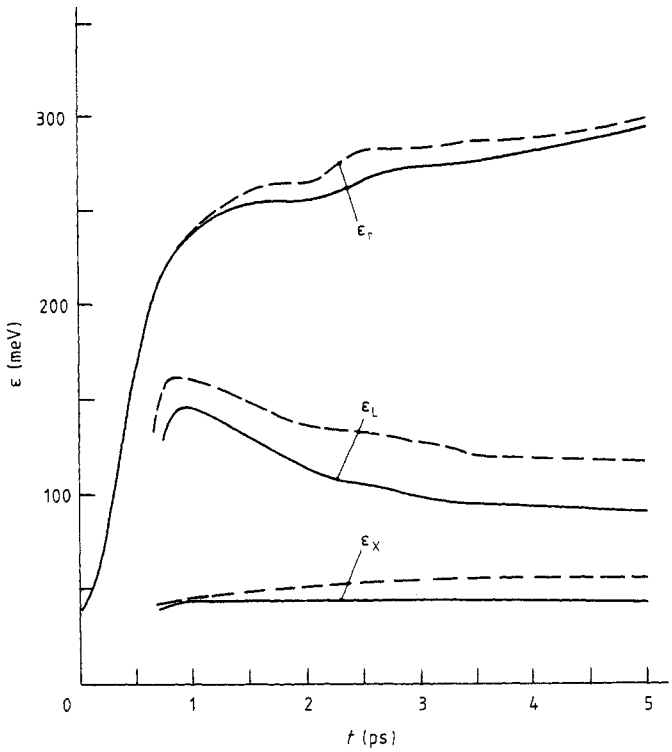

Figure 9. Transient response of the mean electron energy in the Γ, L, X valleys. Full curves: without hot phonons; broken curves: with hot phonons. $T = 300$ K, $n_i = 0$, $n = 5 \times 10^{17}$ cm^{-3}, $E = 10$ kV cm^{-1}.

Figure 11 represents the steady-state velocity-field characteristics at various conditions. Hot phonons yield the lower threshold fields for the electron inter-valley transfer and negative differential mobility.

4. Conclusions

We have obtained that the electrons heated by electric fields generate the forward-displaced non-equilibrium phonon distributions in momentum space even at moderate electron concentrations. The phonon 'heating' dynamics consists of two stages. During the first one the maximum phonon occupation number reaches the near-saturation value. The second stage is associated with the phonon redistribution in momentum space (non-equilibrium phonon distribution broadening).

Hot phonon influences on the electron high-field transport in GaAs are determined by the competition of two velocity reducing and two velocity increasing effects. The velocity decrease is a result of (i) the electron diffusive heating due to the electron scattering by non-equilibrium phonons and (ii) the hot-phonon-induced inter-valley transfer amplification due to the mean electron energy increase. The velocity increasing mechanisms are (i) the hot phonon induced electron 'runaway' from the ionised impurity scattering due to the mean energy increase and (ii) the hot phonon drag effect. The hot

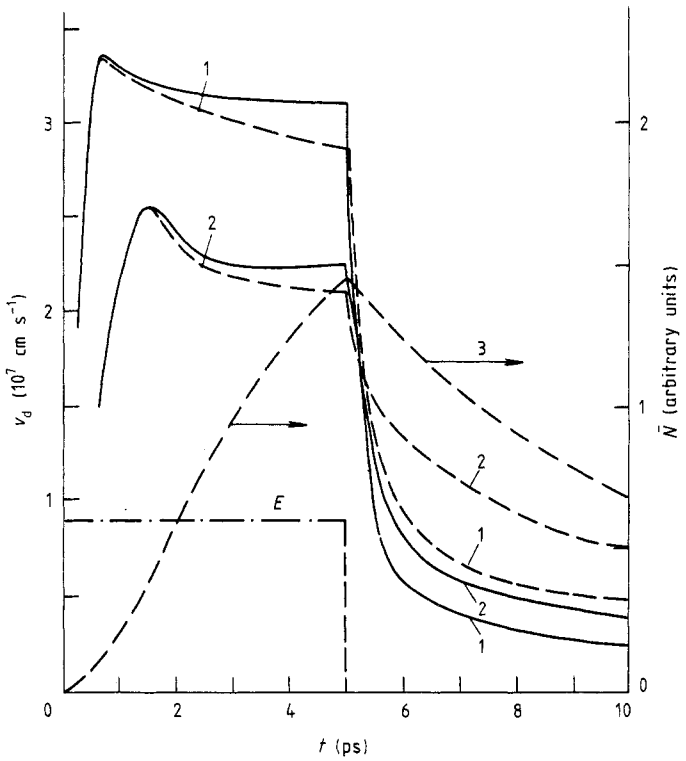

Figure 10. Transient response to a square electric field pulse of the electron drift velocity (left scale) and the average non-equilibrium phonon population (right scale). Curve 1: E = 3 kV cm^{-1}, curve 2: E = 1 kV cm^{-1}. Full curves: without hot phonons, broken curves: with hot phonons. T = 77 K, n_i = 0, n = 10^{17} cm^{-3}.

phonon drag is caused by the electron drift momentum increase due to the interaction with the non-equilibrium phonons forward displaced in momentum space. At various conditions all these effects manifest themselves in a different way.

At low temperatures in pure GaAs the electron diffusive heating is dominant due to the narrow electron distribution in momentum space. Therefore, the hot phonon drag regime is not achieved even at fields as low as 1 kV cm^{-1}.

At room temperature in pure GaAs the hot phonon drag is dominant up to fields of 2 kV cm^{-1}. At higher fields the inter-valley transfer amplification plays the main role leading to the decrease of the drift velocity.

The competition between velocity increasing and decreasing mechanisms yields under certain conditions (pure GaAs, E = 2–3 kV cm^{-1}, T = 300 K) the hot-phonon-induced electron velocity overshoot.

In doped GaAs the hot-phonon-stimulated energy increase and 'runaway' from impurity scattering plays the dominant role up to the threshold fields of the inter-valley transfer. This yields the increase of the electron drift velocity.

At fields of the order of 10 kV cm^{-1}, where the electron inter-valley scattering is dominant, the hot phonon effect on the electron transient characteristics is insignificant. Hot phonons lead to the electron redistribution between the L and X valleys and to the resulting decrease of the stationary drift velocity.

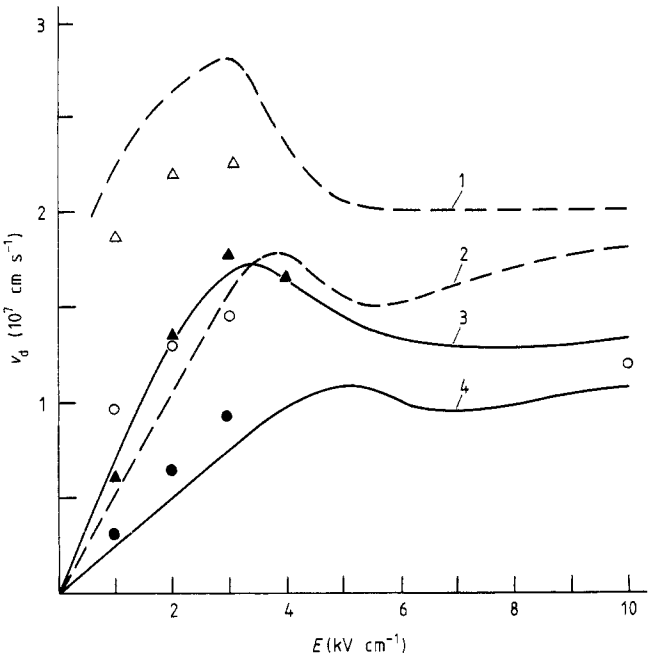

Figure 11. Steady-state velocity-field characteristics. $T = 77$ K: curve 1 and △: $n_i = 0$; curve 2 and ▲: $n_i = 10^{17}$ cm^{-3}; $T = 300$ K: curve 3 and ○: $n_i = 0$; curve 4 and ●: $n_i = 5 \times 10^{17}$ cm^{-3}. Dots and curves are calculated with and without hot phonons, respectively.

Hot phonons affect the relaxation of electron drift velocity after switching off an electric field. The interaction of electrons with the hot phonons 'shifted' in momentum space yields the prolonged relaxation of the electron drift velocity.

Hot phonons influence the electron steady-state characteristics reducing the threshold fields for the electron inter-valley transfer and negative differential mobility.

References

[1] von der Linde D, Kuhl J and Klingenberg H 1980 *Phys. Rev. Lett.* **44** 1505
[2] Collins C L and Yu P Y 1983 *Phys. Rev.* B **27** 2602; 1984 *Phys. Rev.* B **30** 4501
[3] Kash J A, Tsang J C and Hvam J M 1985 *Phys. Rev. Lett.* **54** 2151
[4] Shah J, Pinczuk A, Gossard A C and Wiegmann W 1985 *Physica* B **134** 174
[5] Kash K, Shah J, Block D, Gossard A C and Wiegmann W 1985 *Physica* B **134** 189
[6] Kash J A and Tsang J C 1988 *Solid State Electron.* **31** 419
[7] Shum K, Junnarkar M R, Chao H S, Alfano R R and Morkoc H 1988 *Solid State Electron.* **31** 451
[8] Lugli P, Jacoboni C, Reggiani L and Kocevar P 1987 *Appl. Phys. Lett.* **50** 1251
[9] Lugli P 1987 *Phys. Scr.* T **19A** 190
[10] Lugli P 1988 *Solid State Electron.* **31** 667
[11] Mickevičius R and Reklaitis A 1987 *Solid State Commun.* **64** 1305
[12] Mickevičius R and Reklaitis A 1988 *Phys. Status Solidi* b **150** 437
[13] Pötz W, Osman M A and Ferry D K 1988 *Solid State Electron.* **31** 673
[14] Kočevar P 1972 *J. Phys. C: Solid State Phys.* **5** 3349
[15] Kočevar P 1985 *Physica* B **134** 155
[16] Rieger M, Kocevar P, Bordone P, Lugli P and Reggiani L 1988 *Solid State Electron.* **31** 678
[17] Aspnes D E 1976 *Phys. Rev.* B **14** 5331

[18] Mickevičius R and Reklaitis A 1989 *Semicond. Sci. Technol.* at press
[19] Mickevičius R and Reklaitis A 1986 *Fiz. Tekh. Poluprovodn.* **20** 1693
[20] Klemens P G 1966 *Phys. Rev.* **148** 845
[21] Menendez J and Cardona M 1984 *Phys. Rev.* B **29** 2051
[22] Požela J and Reklaitis A 1980 *Solid State Electron.* **23** 927